Research Article

Journal of Molecular Recognition

Received: 18 June 2009, Revised: 8 July 2009, Accepted: 9 July 2009, Published online in Wiley InterScience: 19 August 2009

(www.interscience.wiley.com) DOI:10.1002/jmr.979

A loop in the *N*-lobe of human serum transferrin is critical for binding to the transferrin receptor as revealed by mutagenesis, isothermal titration calorimetry, and epitope mapping

Anne B. Mason[a]*, Shaina L. Byrne[a], Stephen J. Everse[a], Samantha E. Roberts[a], N. Dennis Chasteen[b], Valerie C. Smith[c], Ross T. A. MacGillivray[c], Banu Kandemir[d] and Fadi Bou-Abdallah[d]

Transferrin (TF) is a bilobal transport protein that acquires ferric iron from the diet and holds it tightly within the cleft of each lobe (thereby preventing its hydrolysis). The iron is delivered to actively dividing cells by receptor mediated endocytosis in which diferric TF preferentially binds to TF receptors (TFRs) on the cell surface and the entire complex is taken into an acidic endosome. A combination of lower pH, a chelator, inorganic anions, and the TFR leads to the efficient release of iron from each lobe. Identification of residues/regions within both TF and TFR required for high affinity binding has been an ongoing goal in the field. In the current study, we created human TF (hTF) mutants to identify a region critical to the interaction with the TFR which also constitutes part of an overlapping epitope for two monoclonal antibodies (mAbs) to the *N*-lobe, one of which was previously shown to block binding of hTF to the TFR. Four single point mutants, P142A, R143A, K144A, and P145A in the *N*-lobe, were placed into diferric hTF. Isothermal titration calorimetry (ITC) revealed that three of the four residues (Pro142, Lys144, and Pro145) in this loop are essential to TFR binding. Additionally, Lys144 is common to the recognition of both mAbs which show different sensitivities to the three other residues. Taken together these studies prove that this loop is required for binding of the *N*-lobe of hTF to the TFR, provide a more precise description of the role of each residue in the loop in the interaction with the TFR, and confirm that the *N*-lobe is essential to high affinity binding of diferric hTF to TFR.

Keywords: human serum transferrin; isothermal titration calorimetry; binding isotherms; transferrin receptor; epitope; recombinant protein; BHK cells; His-tag

INTRODUCTION

The transferrins (TF) are a family of proteins that play a critical role in iron homeostasis (Mason and Everse, 2008). Members of the TF family are comprised of a single polypeptide chain of ~680 amino acids, with a mass of ~80 kDa, which folds into two homologous lobes, designated the *N*- and *C*-lobes. In the specific case of human serum TF (hTF), the lobes are connected by a short (7 amino acid) linker (Wally *et al*., 2006). Each lobe is further divided into two subdomains (NI/NII and CI/CII), that define a cleft in which a single ferric iron is tightly bound in a distorted octahedral coordination. Within each cleft of hTF, the iron is held by the side chains of four amino acids (two tyrosines, and single histidine and aspartic acid residues), in addition to two oxygen

* *Correspondence to: A. B. Mason, Department of Biochemistry, College of Medicine, University of Vermont, 89 Beaumont Avenue, Burlington, VT 05405, USA. E-mail: anne.mason@uvm.edu*

a *A. B. Mason, S. L. Byrne, S. J. Everse, S. E. Roberts*
Department of Biochemistry, College of Medicine, University of Vermont, 89 Beaumont Avenue, Burlington, VT 05405, USA

b *N. D. Chasteen*
Department of Chemistry, University of New Hampshire, Parsons Hall, Durham, NH 03824, USA

c *V. C. Smith, R. T. A. MacGillivray*
Department of Biochemistry and Molecular Biology and Centre for Blood Research, University of British Columbia, Vancouver, BC V6T 1Z3, Canada

d *B. Kandemir, F. Bou-Abdallah*
Department of Chemistry, State University of New York at Potsdam, Stowell Hall, Potsdam, NY 13676, USA

Abbreviations: *TF, serum transferrin; hTF, human serum transferrin; Fe_2 hTF, recombinant diferric hTF that contains an N-terminal hexa-His tag and is non-glycosylated; Fe_C hTF, recombinant monoferric C-lobe hTF (mutations Y95F and Y188F preclude iron binding in the N-lobe) that contains an N-terminal hexa-His tag and is non-glycosylated; Fe_N hTF, recombinant monoferric N-lobe hTF (mutations Y426F and Y517F preclude iron binding in the C-lobe) that contains an N-terminal hexa-His tag and is non-glycosylated; P142A, R143A, K144A, and P145A refer to single point mutants of hTF placed in the Fe_2 hTF background; TFR, transferrin receptor; sTFR, glycosylated soluble portion of the transferrin receptor (residues 121–760) expressed as a recombinant entity that contains an N-terminal hexa-His tag; BHK, baby hamster kidney cells; mAb, monoclonal antibody; ELISA, enzyme linked immunosorbant assay; BSA, bovine serum albumin; ITC, isothermal titration calorimetry; HRP, horseradish peroxidase; TMB, 3,3′,5,5′-tetramethylbenzidine.*

atoms from a carbonate anion. This carbonate is referred to as the synergistic anion due to its essential role in high affinity binding of the ferric iron. In the absence of a synergistic anion the ferric iron becomes hydrolyzed and insoluble.

Diferric hTF binds with high specificity and high affinity to receptors located on the surface of actively dividing cells (Klausner *et al*., 1983; Morgan, 1983; Young *et al*., 1984). TF binds to the large extracellular domain of the TF receptor (TFR) which extends into the extracellular milieu and is connected by a single transmembrane region to a short *N*-terminal region projecting into the cytoplasm. Following endocytosis of the complex, iron is released within the endosome by a combination of lower pH, an unidentified chelator, participation of inorganic anions and the TFR. The extracellular domain of the TFR has been produced recombinantly as a soluble entity (sTFR). Crystal structures of the soluble portion alone (Lawrence *et al*., 1999), or in complex with HFE (the hemochromatosis gene product) (Lebron *et al*., 1998) are available. The structures reveal that the soluble portion of the TFR is comprised of a central helical portion (responsible for dimerization), a protease-like domain and an apical domain.

Specific regions of the TFR which interact with hTF have been identified through mutagenesis of residues in the TFR in combination with surface plasmon resonance to determine binding affinities (as a function both of pH and of iron content) (Giannetti *et al*., 2003). Seven residues in the TFR with a moderate effect on binding to diferric hTF at pH 7.4 were identified (including Tyr123, Trp124, and Asp125 in the protease-like domain of sTFR). Subsequent work (Giannetti *et al*., 2005) further characterized a double mutant of sTFR, W641A/ F760A; these two residues comprise a hydrophobic patch that binds to hTF and is involved in the pH induced conformational change which ultimately results in the release of iron from the *C*-lobe. This study illustrated that a binding event far from the iron site could influence iron release, highlighting the dynamic nature of the process.

Additional amino acids and/or regions in each lobe of hTF that may be involved in binding to the TFR have been tentatively identified by a low resolution (7.5 Å) cryo-EM model of the TF-sTFR complex (Cheng *et al*., 2004), from radiation foot printing protection assays (Liu *et al*., 2003; Xu *et al*., 2005), and from mutagenesis studies (Giannetti *et al*., 2005). As reviewed (Wally *et al*., 2006), there are convincing data to support some of the suggestions while others seem less likely. In the specific case of the *N*-lobe, four residues in a loop in the NII subdomain (Pro142-Arg143-Lys144-Pro145), appear to make contact with Leu122-Tyr123-Trp124-Asp125 in the sTFR (Cheng *et al*., 2004). Indirect support for this suggestion comes from the fact that these amino acids in the NII subdomain are completely conserved in the TFs that bind to the human TFR and are not well conserved in the TFs that do not (Table 1) (Wally *et al*., 2006). However, direct chemical evidence for the involvement of these hTF residues in the interaction with the TFR has been lacking.

An indirect approach to locating regions of hTF critical to TFR binding is identification of neutralizing monoclonal antibodies (mAbs) specific to the *N*- or *C*-lobe. The ability of such antibodies to block binding of hTF to the TFR on the cell surface combined with identification of the epitopes recognized by such antibodies provides important information. Using this approach, we bracketed the region of a sequential epitope lying in a region between residues 365-401 (most likely between 365 and 385) in the *C*-lobe of hTF for a mAb designated F11 (Teh *et al*., 2005).

Table 1. Comparison of human and nonhuman TF sequences[a]

Human numbering	132	133	134	135	136	137	138	139	140	141	142	143	144	145	146	147	148	149	150	151	152	153
Human TF	I	G	L	L	Y	C	D	L	P	E	P	R	K	P	L	E	K	A	V	A	N	F
Rabbit TF	I	G	L	L	Y	C	D	L	P	E	P	R	K	P	L	E	K	A	V	A	S	F
Rat TF	I	G	L	L	F	C	N	L	P	E	P	R	K	P	L	E	K	A	V	A	S	F
Pig TF	M	G	L	L	Y	D	Q	L	P	E	P	R	K	P	I	E	K	A	V	A	S	F
Bovine TF	M	A	K	L	Y	K	E	L	P	D	P	Q	E	S	I	Q	R	A	A	A	N	F
Mouse TF	I	G	L	L	F	C	K	L	S	E	P	R	S	P	L	E	K	A	V	S	S	F
Horse TF	I	G	L	L	Y	W	Q	L	P	E	P	R	E	S	L	Q	K	A	V	S	N	F
Chicken TF											G	I	E	S								

[a] The first four transferrins with conserved residues 142–145 bind to the human transferrin receptor; the remaining four do not. The mAb HTF.14 recognizes only human TF and pig TF (weakly) in a solution-based competition assay. In an ELISA format, it recognizes human well and pig, rabbit and rat TF moderately well. DB2 recognizes only human TF in a solution-based competition assay. In an ELISA, DB2 recognizes human TF well, rabbit, and rat TF moderately well and pig TF very poorly. Neither mAb binds to bovine, mouse, horse, or chicken TF (or to human lactoferrin). The shaded area indicates the four residues that were mutated in this work. The critical lysine residue at position 144 is shown in blue. Residues shown in red are not conserved in human TF.

Journal of Molecular Recognition

In the present work, we have produced single point mutants of the four residues which reside in the *N*-lobe of hTF (P142A, R143A, K144A, and P145A) and which, as indicated above, have been implicated in binding to the TFR. Each mutant was placed into a nonglycosylated diferric construct, recombinant diferric hTF that contains an *N*-terminal hexa-His tag and is non-glycosylated (Fe_2 hTF) (Mason *et al*., 2004). The ability of each mutant, in comparison to the control Fe_2 hTF, to bind to the sTFR has been evaluated by isothermal titration calorimetry (ITC) measurements. In quantifying the concentration of these mutants in the tissue culture medium of our mammalian expression system, we found that two mAbs to the *N*-lobe (designated HTF.14 and DB2) reported unexpectedly low concentrations for some mutants relative to the F11 mAb that is specific to the *C*-lobe. In the current study, we document this finding and investigate the nature of the overlapping epitope for these two *N*-lobe antibodies. We review what is known about these particular mAbs and how this enhances our understanding of the hTF/TFR interaction. These approaches combine to unequivocally identify the residues in the *N*-lobe of hTF that are crucial to its interaction with the TFR.

MATERIALS AND METHODS

Materials

Dulbecco's modified Eagle's medium-Ham F-12 nutrient mixture, antibiotic–antimycotic solution (100x), and trypsin were from the GIBCO-BRL Life Technologies Division of Invitrogen. Fetal bovine serum was obtained from Atlanta Biologicals. Ultroser G is a serum replacement from Pall BioSepra (Cergy, France). The QuikChange mutagenesis kit and pBluescriptII came from Stratagene. Methotrexate from Bedford laboratories was used for selection of plasmid containing baby hamster kidney (BHK) cells. All Corning tissue culture dishes, flasks, and expanded surface roller bottles were obtained from local distributors as were Ultracel 30 kDa MWCO microcentrifuge devices (Amicon). Hi-prep 26/60 Sephacryl S-200HR and S-300HR columns were obtained from Amersham Pharmacia. Ni-NTA resin came from Qiagen, EDTA from the Mann Research Laboratories Inc, the 3,3′,5,5′-tetramethylbenzidine (TMB) Microwell peroxidase substrate system from Kirkegaard and Perry Laboratories (Gaithersburg, MD) and rabbit anti-mouse immunoglobulin G (IgG) from Southern Biological Associates. NTA and ferrous ammonium sulfate were from Sigma, immunopure NHS-LC-biotin and immunopure avidin-horseradish peroxidase (HRP) from Pierce and Removawells (immulon 1 B flat bottom 1 × 12 strips) from Fisher Scientific.

Monoclonal antibodies

The mAb, designated DB2, which we found to be specific to the *N*-lobe, was generously donated by Dade Behring (Marburg, Germany). A second mAb to the *N*-lobe, designated HTF.14 was purchased from Exbio Praha (Czechoslovakia). As described in detail, two other antibodies specific to the *N*-lobe and designated, $HT+N_1$ and $HT+N_2$, were prepared in our laboratory (Mason and Woodworth, 1991). Also as described previously, the F11 mAb to the *C*-lobe, was isolated from ascites fluid kindly provided by Dr James Cook and coworkers (University of Kansas Medical Center, Kansas City, KS) (Mason and Woodworth, 1991).

Production of hTF single-point mutants and the sTFR

Mutations were introduced into the pNUT construct containing the cDNA coding for Fe_2 hTF using the quikchange site-directed mutagenesis kit as described in detail previously (Halbrooks *et al*., 2003). The forward mutagenic primers used to create the single-point mutants with the nucleotides highlighted in bold indicating the substitutions resulting in the mutation are listed below:

P142A Forward

5′-AC TGT GAC TTA CCT GAG **G**CA CGT AAA CCC CTT GAG AAA GCA GTG G-3′

R143A Forward

5′-AC TGT GAC TTA CCT GAG CCA **GC**T AAA CCT CTT GAG AAA GCA GTG G-3′

K144A Forward

5′-AC TGT GAC TTA CCT GAG CCA CGT **GC**A CCT CTT GAG AAA GCA GTG G-3′

P145A Forward

5′-AC TGT GAC TTA CCT GAG CCA CGT AAA **GC**C CTT GAG AAA GCA GTG G-3′

For each construct, the presence of the correct mutation was confirmed by DNA sequence analysis of the cDNA insert and the plasmid flanking regions within 300 bp of the cloning sites.

Transfection of the plasmid into BHK cells followed by selection with methotrexate resulted in secretion of recombinant hTF and mutants of hTF into the tissue culture medium (Mason *et al*., 2004). As described in detail (Mason *et al*., 2001), $Fe^{3+}(NTA)_2$ was added to the tissue culture medium immediately upon collection to iron load and thereby stabilize the recombinant hTF throughout the purification process. The volume of the collected medium was reduced using a tangential flow device with a 30 kDa cutoff membrane. The concentrated medium was centrifuged (6000× g) to remove particulates and the supernatant was diluted by addition of 5× Qiagen start buffer to the sample to yield a 1× final concentration of 50 mM Tris, pH 7.5, 300 mM NaCl, 20 mM imidazole, 10% glycerol and 0.05% sodium azide. The His-tagged Fe_2 hTF control and the mutants were captured by passage over a Qiagen Ni-NTA column and displaced from the column by addition of 250 mM imidazole to the 1× Qiagen start buffer. Passage over Sephacryl S-200HR gel filtration column in 100 mM NH_4HCO_3 completed the purification. As described below, a competitive immunoassay was used to monitor protein production. SDS-PAGE on 10% gels was used to confirm the homogeneity of the samples. The His-tagged sTFR was produced and purified using the same expression system and purification protocol (Byrne *et al*., 2006).

Binding affinity measurements by isothermal titration calorimetry (ITC)

The thermodynamics of the Fe_2 hTF and mutants binding to the sTFR were carried out at pH 7.4 (100 mM Mops, containing 50 mM NaCl and 50 mM $NaHCO_3$) and 25°C using an upgraded CSC model 4200 isothermal titration calorimeter (Calorimetry Science Corporation, Provo, Utah). The instrument operation, settings, and calibration were performed as described elsewhere (Bou-Abdallah *et al*., 2002). Typically, an automated sequence of 25 injections, each of 10 μl titrant into the sample cell, spaced at 5 min intervals to allow complete equilibration, were performed. In ITC experiments, both hTF and sTFR are free in solution. The standard enthalpy change (ΔH°), the binding constant (K), and the stoichiometry of binding (n) are determined by a single ITC experiment. From these values, the standard Gibbs free energy

change (ΔG°), and standard entropy change (ΔS°) are calculated, such that all thermodynamic parameters are defined from a single experiment. The data were collected automatically and analyzed using BindWorks 3.0 fitting program (Calorimetry Science Corporation).

Solution-based competition assay to determine the concentration of recombinant hTF

The competitive immunoassay routinely used in our laboratory has been described in detail previously (Mason *et al.*, 2001). Briefly, removawells are coated with rabbit anti-mouse IgG (1 μg/100 μl) to capture a mAb specific for the *N*- or the *C*-lobe of hTF. Biotinylated hTF is added (10 ng/200 μl) in the presence of unlabeled standards and samples. A tube with no added unlabeled hTF establishes the maximum amount of bound biotinylated hTF (B_{100}) and wells with no added specific mAb determine the amount of biotinylated hTF that is nonspecifically bound (B_0). A standard curve is generated by competition of biotinylated hTF with six different amounts of unlabeled hTF (16–400 ng/well). Following washing, an avidin-HRP conjugate is added to all wells. The amount of biotinylated sample that is bound is determined using a TMB substrate system. All steps are carried out in buffer composed of 50 mM Tris-HCl, pH 7.4, containing 100 mM NaCl and 0.1% bovine serum albumin (BSA).

Enzyme-linked immunosorbent assay (ELISA)

Another assessment of the ability of mAbs to recognize both the hTF mutants and TFs of various species is to bind them directly to wells of an assay plate (Church *et al.*, 1988; Mason and Woodworth, 1991). Each TF (1 μg) in 14 mM Na_2CO_3, 34 mM $NaHCO_3$ was bound to uncoated removawells. Following incubation overnight at 4°C, the wells were washed and blocked by addition of 1% BSA in assay buffer. Following washing, addition of each antibody, and incubation for 1 h at 37°C, anti-mouse IgG conjugated to HRP was added to allow visualization of the amount of bound antibody using the TMB substrate system.

Direct competitive assay to determine overlap of mAbs, HTF.14, and DB2

A competitive assay (Stahli *et al.*, 1983; Mason and Woodworth, 1991) was used to determine whether the mAbs to the *N*-lobe were to the same or to different epitopes. In this assay, a ~4-fold excess of a competing mAb (designated mAb2) was pre-incubated with biotinylated hTF and then added to wells coated with the first mAb (mAb1). If the two mAbs were to the same (or nearly the same) epitope, mAb2 would inhibit binding of the biotinylated hTF to mAb1. Controls included biotinylated hTF and no mAb2, use of the same mAb for mAb1 and mAb2 and use of an antibody to the *C*-lobe.

RESULTS

ITC measurements of controls (Fe_2 hTF, Fe_N hTF, and Fe_C hTF) and the four N-lobe mutants in the Fe_2 hTF background binding to the sTFR

The first set of ITC experiments measured the interaction of the recombinant Fe_2 hTF and the two monoferric controls with the sTFR. Representative ITC profiles for these measurements are presented in Figure 1; the main panel displays the raw calorimetric data and the inset shows a plot of the total heat generated per injection as a function of the molar ratio of hTF to sTFR monomer. Note that in solution sTFR always exists as a dimer in which each monomer binds a single molecule of hTF. All binding isotherms were fit with a model corresponding to one set of independent binding sites of hTF with the sTFR. The solid smooth lines in Figure 1 are the best fit of the experimental data with the stoichiometry (*n*), association constant (*K*), standard enthalpy changes (ΔH°), standard entropy changes (ΔS°), and standard free energy of binding (ΔG°) reported in Table 2. In all cases, the

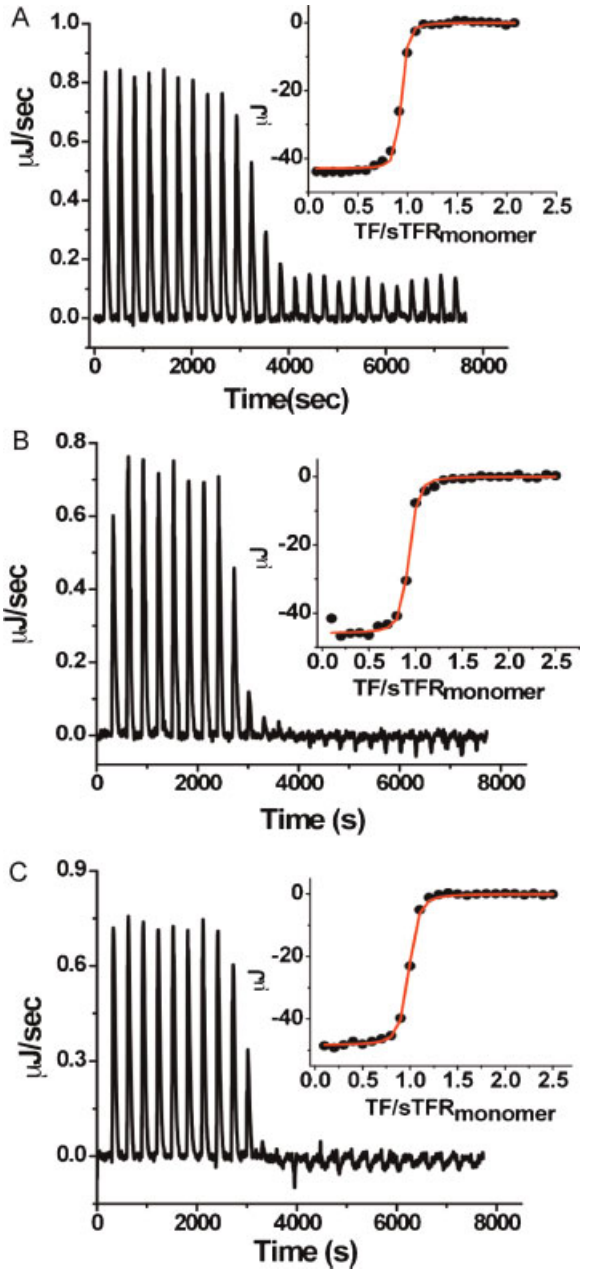

Figure 1. Calorimetric titration (raw data) of (A) Fe_2 hTF, (B) Fe_C hTF, and (C) Fe_N hTF with the sTFR. Insets: plot of the integrated heat versus the TF/$TFR_{monomer}$ ratio. Conditions: (A) 130 μM hTF titrated with 10 μl injections of 12 μM sTFR; (B) and (C) 260 μM hTF titrated with 10 μl injections of 20 μM sTFR. All proteins were in 100 mM Mops, pH 7.4 containing 50 mM NaCl, 50 mM $NaHCO_3$ buffer, and 25°C.

Journal of Molecular Recognition

Table 2. ITC results[a]

Protein	*n* (per sTFR monomer)	K (M^{-1})	ΔH° (KJ/mol)	ΔS° (J/K mol)[b]	ΔG° (KJ/mol)[c]	K_d (nM)[d]
Fe_2 hTF Control	0.98 ± 0.01	$(2.4 \pm 1.3) \times 10^8$	-33.0 ± 0.3	49.6 ± 4.5	-47.8 ± 1.3	4 ± 2
Fe_C hTF Control	0.92 ± 0.01	$(3.1 \pm 1.7) \times 10^7$	-17.4 ± 0.7	85.1 ± 1.5	-42.8 ± 1.3	32 ± 17
Fe_N hTF Control	0.98 ± 0.01	$(2.8 \pm 1.2) \times 10^7$	-18.3 ± 0.2	81.0 ± 1.0	-42.5 ± 1.0	36 ± 15
P142A Fe_2 hTF	0.89 ± 0.01	$(3.8 \pm 2.0) \times 10^7$	-27.6 ± 0.7	52.6 ± 1.5	-43.3 ± 1.3	26 ± 14
R143A Fe_2 hTF	0.96 ± 0.01	$(5.7 \pm 2.4) \times 10^8$	-19.9 ± 0.2	100.9 ± 1.1	-50.0 ± 1.0	2 ± 1
K144A Fe_2 hTF	0.95 ± 0.01	$(4.3 \pm 1.7) \times 10^7$	-19.4 ± 0.3	81.0 ± 1.0	-43.6 ± 1.0	23 ± 10
P145A Fe_2 hTF	0.93 ± 0.01	$(3.5 \pm 1.9) \times 10^7$	-23.5 ± 0.5	65.4 ± 1.4	-43.0 ± 1.3	29 ± 15

[a] The reported thermodynamic parameters are apparent values and include the contributions to the overall equilibrium from hTF, sTFR, and buffer species in different states of protonation. Uncertainties in the thermodynamic parameters *n*, *K*, and ΔH° and are standard errors obtained from the ITC fitting software, Bindworks 3.0. Uncertainties in ΔS°, ΔG°, and K_d were derived from propagation of errors.
[b] Calculated from $\Delta S^\circ = (\Delta H^\circ - \Delta G^\circ)/T$.
[c] Calculated from $\Delta G^\circ = -RT\ln K$.
[d] Calculated from $K = 1/K_d$.

raw ITC data showed exothermic peaks (upward spikes). As the titration progressed, the exothermic peaks decreased in magnitude, as expected for the increased occupancy of sTFR sites by hTF, until heats of dilution corresponding to the interaction of hTF in buffer alone were reached. The results of the complete analysis of these samples are provided in Table 2. The binding constants (*K*) for the interaction between Fe_2 hTF and Fe_N hTF (or Fe_C hTF) with sTFR were $\sim 2 \times 10^8$ and $3 \times 10^7\ M^{-1}$, respectively.

The second set of experiments measured the interaction of the *N*-lobe mutants (P142A, R143A, K144A, and P145A) in the Fe_2 hTF background with the sTFR. With the exception of R143A, the mutants displayed a reduced binding affinity ($K \sim 4 \times 10^7\ M^{-1}$) similar to that of the monoferric hTF controls, indicating that the *N*-lobe residues Pro142, Lys144, and Pro145 are absolutely essential for strong binding of the *N*-lobe of hTF to the sTFR (Figure 2, Table 2). All binding isotherms were fit with a model corresponding to one set of independent binding sites of hTF with sTFR. The solid smooth lines in the insets of Figure 2 are the best fits of the experimental data. The resultant stoichiometries (*n*), binding constants (*K*), standard enthalpy changes (ΔH°), standard entropy changes (ΔS°), and standard free energies of binding (ΔG°) are reported in Table 2.

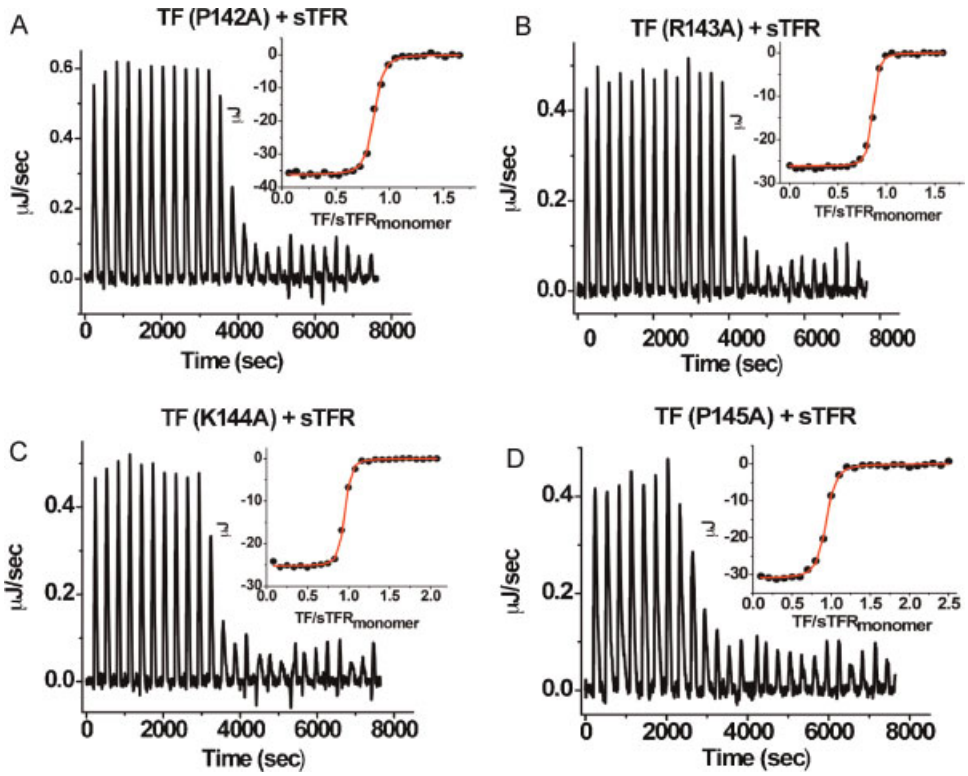

Figure 2. Calorimetric titration (raw data) of (A) P142A, (B) R143A, (C) K144A, and (D) P145A *N*-lobe mutants of Fe_2 hTF with the sTFR. Insets: plot of the integrated heat versus the TF/$TFR_{monomer}$ ratio. Conditions: 130 µM hTF titrated with 10 µl injections of 10–15 µM sTFR. All proteins were in 100 mM Mops, pH 7.4 containing 50 mM NaCl, 50 mM $NaHCO_3$ buffer, and 25°C.

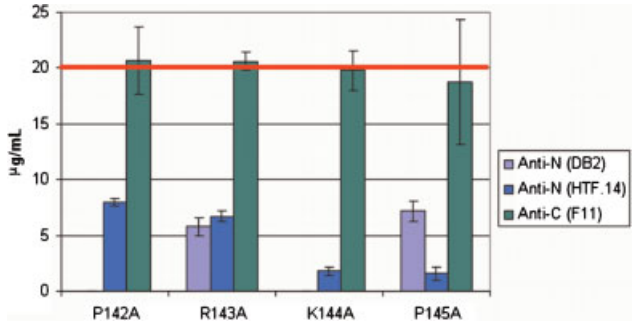

Figure 3. Sensitivity of the four *N*-lobe mutants to mAbs specific to the *N*- or *C*-lobe. The P142A, R143A, K144A, and P145A hTF mutants in the Fe_2 hTF background were made up at a nominal concentration of 20 μg/ml (determined by absorbance measurements) and competed in a solid phase assay format against biotinylated Fe_2 hTF for binding to three mAbs, two specific to the *N*-lobe, DB2, and HTF.14 and one specific to the *C*-lobe, F11 as indicated in the legend on the figure.

Sensitivity of the four N-lobe mutants to mAbs specific to the N- or C-lobe

The P142A, R143A, K144A, and P145A mutants were specifically produced to definitively establish their role in binding to the sTFR. In carrying out the competitive immunoassay, we observed that two mAbs to the *N*-lobe (designated HTF.14 and DB2) gave unexpectedly low concentrations for some of the mutants relative to the mAb specific to the *C*-lobe (F11). To document this finding, we prepared and assayed aliquots of the P142A, R143A, K144A, and P145A hTF mutants, each at a nominal concentration of 20 μg/ml (determined by absorbance measurements). As shown in Figure 3, when the mAb specific to the *C*-lobe is the capturing mAb, all of the samples yielded the expected concentration of 20 μg/ml (within experimental error). In contrast, use of either mAb to the *N*-lobe gave very different results for each mutant. HTF.14 recognized all four mutants, but at a significantly reduced level ranging from a low of 1.6μg/ml for the P145A mutant to a high of 8.0 μg/ml for the P142A mutant. In contrast, DB2 completely failed to recognize the hTF mutants containing either the P142A mutation or the K144A mutation whereas the R143A and P145A mutants yielded 5.8 and 7.2 μg/ml, instead of the expected 20 μg/ml.

Evaluation of TF from other species by solution-based competition assay

Using the solution-based competition assay, hTF competed well with biotinylated hTF for binding to HTF.14. In contrast, pig TF competed weakly such that the assay measured only 2.5 μg/ml for a nominal 20 μg/ml concentration of pig TF (data not shown). Rat and rabbit TF did not compete with biotinylated hTF at all. DB2 only recognized hTF; rat, rabbit, and pig TF were unable to compete with biotinylated hTF. In addition horse, mouse, bovine, and chicken TF and human lactoferrin, proteins which do not bind to the human sTFR, did not compete with biotinylated hTF for binding to either mAb (data not shown).

Evaluation of the ability of HTF.14 and DB2 to bind to the four N-lobe mutants and to TF from other species as determined by ELISA

To further assess the two mAbs, we carried out an ELISA in which the various TFs were directly bound to uncoated wells. As shown in Figure 4, in this noncompetitive format, HTF.14 bound to human, rabbit, rat, and pig TF and to three of the four mutants almost equally well. Thus, if hTF with an A_{450} of 1.357 is taken as 100% binding, by comparison rat TF showed 68% binding, and rabbit TF and pig TF showed 63% binding. Similar values were obtained for all of the mutants except the P145A mutants which had $<$ 50% binding in comparison to the control. DB2 bound to hTF with an A_{450} of 1.099. If that value is assigned as 100% binding, rabbit TF showed 52% binding, rat TF had 44% binding and pig TF only 8% binding. Likewise all of the mutants resulted in a significant decrease in the binding of DB2, with the biggest effect from the P142A (binding at the level of 35%) and P145A (39% binding). Again, we note that neither antibody bound to horse, mouse, bovine, or chicken TF or to human lactoferrin in this format (data not shown).

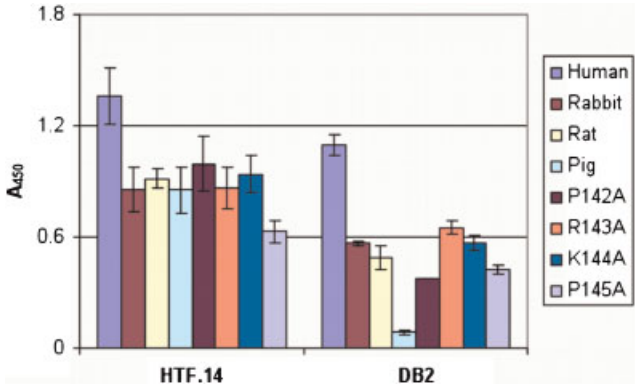

Figure 4. Evaluation of the ability of HTF.14 and DB2 to bind to the four *N*-lobe mutants and to TF from other species as determined by ELISA. Each TF (1 μg) was bound to uncoated removawells. Following incubation overnight at 4°C, the wells were washed and blocked by addition of 1% BSA in assay buffer. Following washing, addition of each mAb, and incubation for 1 h at 37°C, anti-mouse IgG conjugated to HRP was used to allow visualization of the amount of bound antibody using the TMB substrate system.

Direct competition experiment

To investigate the overlap of HTF.14 and DB2, we carried out a direct competitive assay. As shown in Figure 5, the two mAbs very

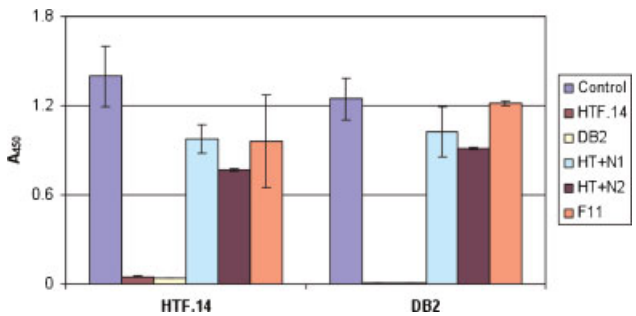

Figure 5. Direct solid phase competitive assay to determine overlap of mAbs, HTF.14 and DB2. Binding of biotinylated Fe_2 hTF pre-incubated with a 4-fold excess of HTF.14 or DB2 to wells containing HTF.14 (or *vice versa*) resulted in an almost complete elimination of binding. Moderate inhibition of two other mAbs to the *N*-lobe ($HT + N_1$ and $HT + N_2$) is observed following pre-incubation (4-fold excess) with the biotinylated Fe_2 hTF and placement into wells pre-coated with either HTF.14 or DB2. The mAb to the *C*-lobe (F11) was similar to the control.

Journal of Molecular Recognition

clearly inhibit each other to a similar extent. Binding of biotinylated Fe_2 hTF pre-incubated with a 4-fold excess of HTF.14 or DB2 to wells containing HTF.14 resulted in $>96\%$ reduction of binding. Complete inhibition (100%) was observed for binding of biotinylated hTF pre-incubated with HTF.14 or DB2 to wells containing DB2. Two other mAbs to the *N*-lobe, $HT+N_1$ and $HT+N_2$, showed a modest amount of inhibition when preincubated at a 4-fold excess with the biotinylated Fe_2 hTF and placed into wells pre-coated with either HTF.14 or DB2. The mAb to the *C*-lobe (F11) was similar to the control, confirming and validating the specificity of this assay.

DISCUSSION

The ITC experiments unequivocally establish that three of the four residues (Pro142, Lys144, and Pro145) in the loop are involved in, and in fact, are crucial to the interaction with the sTFR (Table 2). With the exception of the R143A mutant, the binding affinities of the other Fe2 hTF mutants for the sTFR are about 5–7-fold weaker than that of the control Fe_2 hTF at pH 7.4 (Table 2), implicating Pro142, Lys144, and Pro145 in the loop in high affinity interaction with the sTFR at neutral pH. Mutation of these residues to alanine leads to a *K* more closely resembling the weaker binding of the monoferric controls. It is clear that mutation of these three residues to alanine significantly reduces binding of the *N*-lobe to the sTFR whereas the R143A mutation results in an affinity unchanged from that of the Fe2 hTF control, demonstrating that Arg143 is not required for high affinity binding of the *N*-lobe to the sTFR. The thermodynamic parameters derived from the data in Figures 1 and 2, and presented in Table 2, reveal that the binding of hTF to sTFR is achieved with both favorable enthalpy and entropy changes. As noted in the legend, the reported thermodynamic parameters are apparent values and include the contributions to the overall equilibrium from hTF, sTFR, and buffer species in different states of protonation. Uncertainties in the thermodynamic parameters *n*, *K*, and ΔH° are standard errors obtained from the ITC fitting software and uncertainties in ΔS°, ΔG°, and K_d were derived from propagation of errors.

Overall, the ITC data support the prediction from the cryo-EM model that this loop comprised of residues 142–145 is definitely involved in the interaction with the TFR (Cheng *et al*., 2004), but more precisely defines this interaction by revealing that three of the four residues in the loop are required. The results are also consistent with the finding of Giannetti *et al*. (2003), that mutation of TFR residues Tyr123, Trp124, and Asp125 reduces the interaction with Fe_2 hTF at pH 7.4; in the cryo-EM model these residues appear to be in close proximity to this *N*-lobe loop. Significantly, mutagenesis of these three TFR residues had no effect on the binding of apo-hTF at pH 6.3 (Giannetti *et al*., 2003), indicating that the effect is specific to Fe_2 hTF binding at neutral pH.

The epitopes for HTF.14 and DB2 are conformational as indicated by the failure of these mAbs to recognize hTF (or isolated *N*-lobe) in which the disulfide bonds were reduced (Mason and Woodworth, 1991). Significantly, HTF.14 was also insensitive to the presence or absence of ferric iron in hTF or the isolated *N*-lobe of hTF. The current study shows that, in competition with biotinylated hTF, only hTF was an effective competitor for binding to HTF.14, with pig TF a distant second and no competition by rat or rabbit TF. DB2 was even more specific and selective than HTF.14 since in the solution-based competition assay, only hTF was able to compete. It is also apparent that the mutations in this loop have a significant negative impact on the binding of either mAb, with DB2 displaying the most drastic reduction (Figure 3). The absence of either Pro142 or Lys144 (by mutation to alanine) completely eliminated all binding of DB2 as measured in the competition assay, whereas, loss of Lys144 or Pro145 resulted in the biggest effects on binding of HTF.14. These results indicate that Lys144 is essential to the integrity of the epitope for both mAbs in this format.

In the ELISA format in which 1 μg of each TF was directly bound to the wells of the assay plate, HTF.14 bound best to hTF and moderately (30–40% reduction) to rabbit, rat, and pig TF (Figure 4). HTF.14 did not bind to horse, mouse, chicken, or bovine TF. Three of the four mutants resulted in a similar reduction in binding of HTF.14, with the largest effect from the P145A mutant, in which binding was reduced by half. In the ELISA format, DB2 bound well to hTF whereas binding to rabbit and rat TF was reduced by half and binding to pig TF was below 10%. Likewise binding of DB2 to the four mutants was considerably decreased, 40% for R143A, 50% for K144A, and $>60\%$ reduction for P142A and P145A in comparison to the Fe_2 hTF control.

In spite of the differences in the binding profiles in both assay formats, the epitopes for HTF.14 and DB2 clearly overlap. In the solution-based competition experiment, HTF.14 significantly reduced the amount of biotinylated hTF bound by DB2 and *visa versa* indicating a shared region of the epitope (Figure 5). It is less clear precisely which other residues constitute the epitope for each mAb and contribute to the subtle differences in their specificity; however, an amino acid sequence alignment provides some insights. As shown in Table 1 there is a substantial amount of sequence identity in the immediate vicinity of the loop. The critical nature of Lys144 is supported by the fact that it is not conserved in any of the sequences that are not recognized by HTF.14 and DB2. These include bovine, mouse, and horse and chicken TFs, and human lactoferrin which contain either a serine or a glutamate residue at this position. It is less clear why DB2 recognizes rabbit and rat TF only in the ELISA format and does not bind to pig TF well in either assay since all of these TFs retain the conserved Lys at position 144. We suggest that the substitution of a serine residue at position 152 in place of asparagine might explain the difference in reactivity (at least in part). As shown in Figure 6, Asn152 lies close to Pro142, Lys144, and Pro145 in the X-ray crystal structure. Interestingly, Arg143 which does not reside on the same face is the only residue that does not inhibit binding to the TFR (Table 2). Overall, it is clear that this particular region of the *N*-lobe is surface exposed and hence available to bind to the TFR and to elicit an immune response. It is also interesting to briefly consider the difference in the results from the solid phase competition assay versus the ELISA. Obviously the ELISA format allows access to regions of each antigen which may be more exposed due to the distortions caused by binding to the assay plate. This means that, in the absence of competition by a preferred antigen, even antigens with weaker binding can be detected. In this context, the fact that DB2 does not bind well to pig TF may be due to the changes in the residues at positions 137 and 138 (Table 1).

Collectively, our results attest to the fact that both lobes are required to get very high affinity binding of Fe_2 hTF to the specific TFR at neutral pH. Three of the four *N*-lobe mutants bind with affinities that more closely resemble the monoferric constructs ($K_d \sim 30$ nM) than the Fe_2 diferric construct (K_d 4 nM), indicating that

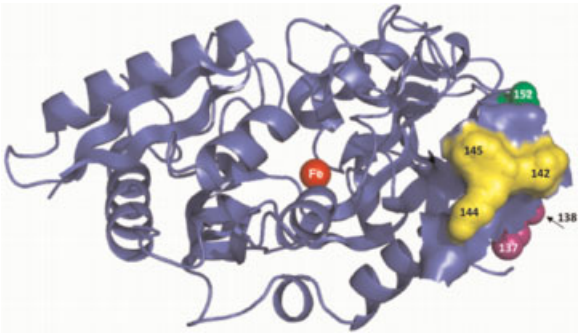

Figure 6. Crystal structure of the *N*-lobe of hTF (PDB 1A8E) showing the location of the residues of interest. Backbone cartoon highlighting the predicted epitope (Pro142, Lys144, and Pro145 yellow) and indicating other residues of interest (Cys137 and Asp138 purple and Asn152 green). A surface is drawn extending 7 Å from Lys144. Iron is shown as a red sphere. Figure prepared using Pymol (Delano, 2002).

the *N*-lobe of the three mutants really does not contribute much to the binding. We note that the binding affinity of each of the monoferric constructs is still considerable because they still have either a functional *C*-lobe or a functional *N*-lobe through which to bind. The ITC results are consistent with the notion that mutation of three of the four residues in the loop to alanine interferes with binding of the *N*-lobe thereby validating part of the cryo-EM model which indicated the proximity of Pro142, Arg143, Lys144, and Pro145 in the NII domain to residues in the protease domain of the TFR. Our previous work (Mason *et al*., 1997) provided compelling evidence that the *N*-lobe in full-length hTF plays a role in the high affinity binding of Fe2 hTF to the TFR. Further proof came from equilibrium binding experiments showing that the free energy of binding of each monoferric hTF was equivalent and, significantly, was not additive (Mason *et al*., 2005). The current work now provides additional irrefutable evidence that both lobes are required for highest affinity binding and that the loop region of the *N*-lobe contributes significantly to this binding. The notion that the isolated *C*-lobe alone (Zak *et al*., 1994) provides most of the binding free energy is not supported and does not adequately take into account the crucial contribution of each lobe in the bilobal structure to both binding and concerted iron release. A K_d of 650 nM for the binding of isolated *C*-lobe to K562 cells (Zak and Aisen, 2002) compares well to a K_d of 800 nM from SPR studies measuring binding of *C*-lobe to a tethered sTFR (Giannetti *et al*., 2003). In the current study (and roughly consistent with the previous SPR estimate for Fe_C hTF of $\sim$60 nM (Giannetti *et al*., 2005)), ITC measurements yielded a K_d of $\sim$30 nM for each monoferric construct. It is very clear that the *N*-lobe substantially enhances the affinity of hTF for the receptor. We are slowly coming to a more comprehensive understanding of the importance in iron release of the interaction between the two lobes of hTF and the TFR (Byrne and Mason, 2009). It is a very complex system and unraveling the effects of lobe–lobe interaction, pH, anions, and the TFR is a huge challenge.

CONCLUSIONS

The combination of mutagenesis, ITC, and epitope mapping of two neutralizing mAbs has revealed important and detailed insights into a loop region of the *N*-lobe, demonstrating that it is a key structural motif which plays a role in high affinity binding of the *N*-lobe of hTF to the TFR, without impacting the binding of the *C*-lobe. The current work provides support for placement of the two lobes of hTF in the Fe_2 hTF/TFR complex as predicted by the cryo-EM model; however, the work gives no insight into the possible origin of the 9 Å shift required to place the lobes relative to each other in that model (Cheng *et al*., 2004).

Acknowledgements

This work was supported by a USPHS Grant R01 DK21739 (ABM) and R37-GM-20194 from the National Institute of General Medical Sciences (to NDC). FBA received funds from the Research and Creative Endeavor Program, SUNY Potsdam, and the Cottrell College Science Award (ID # 7892) from Research Corporation.

REFERENCES

Bou-Abdallah F, Arosio P, Santambrogio P, Yang X, Janus-Chandler C, Chasteen ND. 2002. Ferrous ion binding to recombinant human H-chain ferritin. An isothermal titration calorimetry study. *Biochemistry* **41**: 11184–11191.

Byrne SL, Leverence R, Klein JS, Giannetti AM, Smith VC, MacGillivray RTA, Kaltashov IA, Mason AB. 2006. Effect of glycosylation on the function of a soluble, recombinant form of the transferrin receptor. *Biochemistry* **45**: 6663–6673.

Byrne SL, Mason AB. 2009. Human serum transferrin: a tale of two lobes. Urea gel and steady state fluorescence analysis of recombinant transferrins as a function of pH, time, and the soluble portion of the transferrin receptor. *J. Biol. Inorg. Chem.* **14**: 771–781.

Cheng Y, Zak O, Aisen P, Harrison SC, Walz T. 2004. Structure of the human transferrin receptor-transferrin complex. *Cell* **116**: 565–576.

Church WR, Brown SA, Mason AB. 1988. Monoclonal antibodies to the amino- and carboxyl-terminal domains of ovotransferrin. *Hybridoma* **7**: 471–484.

Delano WL. 2002. The PyMOL Molecular Graphics System. DeLano Scientific: San Carlos, CA, USA.

Giannetti AM, Snow PM, Zak O, Bjorkman PJ. 2003. Mechanism for multiple ligand recognition by the human transferrin receptor. *PLoS Biol.* **1**: 341–350.

Giannetti AM, Halbrooks PJ, Mason AB, Vogt TM, Enns CA, Bjorkman PJ. 2005. The molecular mechanism for receptor-stimulated iron release from the plasma iron transport protein transferrin. *Structure* **13**: 1613–1623.

Halbrooks PJ, He QY, Briggs SK, Everse SJ, Smith VC, MacGillivray RTA, Mason AB. 2003. Investigation of the mechanism of iron release from the C-lobe of human serum transferrin: mutational analysis of the role of a pH sensitive triad. *Biochemistry* **42**(13): 3701–3707.

Klausner RD, van Renswoude J, Ashwell G, Kempf C, Schechter AN, Dean A, Bridges KR. 1983. Receptor-mediated endocytosis of transferrin in K562 cells. *J. Biol. Chem.* **258**: 4715–4724.

Lawrence CM, Ray S, Babyonyshev M, Galluser R, Borhani DW, Harrison SC. 1999. Crystal structure of the ectodomain of human transferrin receptor. *Science* **286**(5440): 779–782.

Lebron JA, Bennett MJ, Vaughn DE, Chirino AJ, Snow PM, Mintier GA, Feder JN, Bjorkman PJ. 1998. Crystal structure of the hemochromatosis protein HFE and characterization of its interaction with transferrin receptor. *Cell* **93**(1): 111–123.

Liu RT, Guan JQ, Zak O, Aisen P, Chance MR. 2003. Structural reorganization of the transferrin C-lobe and transferrin receptor upon complex formation: the C-lobe binds to the receptor helical domain. *Biochemistry* **42**(43): 12447–12454.

Mason AB, Tam BM, Woodworth RC, Oliver RWA, Green BN, Lin LN, Brandts JF, Savage KJ, Lineback JA, MacGillivray RTA. 1997. Receptor recognition sites reside in both lobes of human serum transferrin. *Biochem. J.* **326**: 77–85.

Mason AB, Halbrooks PJ, Larouche JR, Briggs SK, Moffett ML, Ramsey JE, Connolly SA, Smith VC, MacGillivray RTA. 2004. Expression, purification, and characterization of authentic monoferric and apohuman serum transferrins. *Protein Expr. Purif.* **36**(2): 318–326.

Mason AB, Woodworth RC. 1991. Monoclonal antibodies to the amino- and carboxyl-terminal domains of human transferrin. *Hybridoma* **10**: 611–623.

Mason AB, He QY, Adams TE, Gumerov DR, Kaltashov IA, Nguyen V, MacGillivray RTA. 2001. Expression, purification, and characterization of recombinant nonglycosylated human serum transferrin containing a C-terminal hexahistidine tag. *Protein Expr. Purif.* **23**(1): 142–150.

Mason AB, Halbrooks PJ, James NG, Connolly SA, Larouche JR, Smith VC, MacGillivray RTA, Chasteen ND. 2005. Mutational analysis of C-lobe ligands of human serum transferrin:insights into the mechanism of iron release. *Biochemistry* **44**: 8013–8021.

Mason AB, Everse SJ. 2008. Iron transport by transferrin. In Iron Metabolism and Disease, Fuchs H (ed.). Research Signpost: Kerala, India; 83–123.

Morgan EH. 1983. Effect of pH and iron content of transferrin on its binding to reticulocyte receptors. *Biochim. Biophys. Acta* **762**: 498–502.

Stahli C, Miggiano V, Stocker J, Staehelin TH, Haring P, Takacs B. 1983. Methods in Enzymology, Vol. 92. Academic Press: Orlando.

Teh M, Hewitt J, Ung KC, Griffiths TA, Nguyen V, Briggs SK, Mason AB, MacGillivray RTA. 2005. Identification of the epitope of a monoclonal antibody that disrupts binding of human transferrin to the human transferrin receptor. *FEBS J.* **272**(24): 6344–6353.

Wally J, Halbrooks PJ, Vonrhein C, Rould MA, Everse SJ, Mason AB, Buchanan SK. 2006. The crystal structure of iron-free human serum transferrin provides insight into inter-lobe communication and receptor binding. *J. Biol. Chem.* **281**(34): 24934.–24944.

Xu G, Liu R, Zak O, Aisen P, Chance MR. 2005. Structural allostery and binding of the transferrin receptor complex. *Mol. Cell Proteomics* **4**(12): 1959–1967.

Young SP, Bomford A, Williams R. 1984. The effect of the iron saturation of transferrin on its binding and uptake by rabbit reticulocytes. *Biochem. J.* **219**: 505–510.

Zak O, Trinder D, Aisen P. 1994. Primary receptor-recognition site of human transferrin is in the C-terminal lobe. *J. Biol. Chem.* **269**: 7110–7114.

Zak O, Aisen P. 2002. A new method for obtaining human transferrin C-lobe in the native conformation: preparation and properties. *Biochemistry* **41**(5): 1647–1653.

